Published by Avanti Publishers

Journal of Advanced Thermal Science Research

ISSN (online): 2409-5826

A Convolutional-Neural-Network Surrogate for Steady-State Radiative Heating in Thermoforming

Erhan Turan[1], Büryan Apaçoğlu-Turan[1,*] and Alper Sametoğlu[2]

[1]*Simularge A.Ş., Istanbul, Türkiye*

[2]*Earth and Planetary Sciences, ETH Zurich, Zurich, Switzerland*

ARTICLE INFO

Article Type: Research Article

Academic Editor: Dunxi Yu

Keywords:
Digital twin
Thermoforming
Radiative heat transfer
Finite-element simulation
Convolutional neural network

Timeline:
Received: October 05, 2025
Accepted: November 24, 2025
Published: December 22, 2025

Citation: Turan E, Apaçoğlu-Turan B, Sametoğlu A. A convolutional-neural-network surrogate for steady-state radiative heating in thermoforming. J Adv Therm Sci Res. 2025; 12: 73-84.

DOI: https://doi.org/10.15377/2409-5826.2025.12.5

ABSTRACT

Thermoforming is widely used to produce lightweight packaging and durable components, yet controlling the temperature field during the heating stage remains challenging. Finite-element models that capture conduction, convection and diffuse-radiative exchange provide accurate predictions, but their high computational cost precludes real-time optimization and digital-twin deployment. In this study a convolutional-neural-network (CNN) surrogate is developed to predict steady-state temperature distributions for a polymer sheet heated by an array of radiative heaters. A parametric study sampled heater temperature distributions, sheet thicknesses and initial temperatures, and a nonlinear finite-element model was discretized and used to compute steady-state temperature fields. The resulting dataset of input vectors and temperature maps served to train a fully convolutional neural network, whose weights were optimized with the Adam algorithm by minimizing the mean-squared error. On a held-out test set the surrogate achieved a coefficient of determination of 0.96 and a mean relative error less than 3%, while producing predictions in under 1 second—an order-of-magnitude speedup relative to the finite-element solver. Gradient-based inversion of the trained network successfully recovered heater temperature distributions that reproduced target temperature fields, even under simulated heater failures, demonstrating the feasibility of fault-tolerant control. These results show that the proposed CNN surrogate bridges high-fidelity simulation and real-time control, enabling digital-twin implementations for thermoforming and providing a foundation for future extensions to transient heating and experimental validation.

*Corresponding Authors
Email: buryan.turan@simularge.com
Tel: +(90) 5423458714

1. Introduction

Thermoforming is widely used to produce packaging for agricultural products, pharmaceuticals, consumer goods and domestic appliances, as well as durable parts such as aircraft components, material-handling equipment and automotive interior panels. In a typical thermoforming process, a flat polymer sheet is heated above its forming temperature, formed over a mold and then cooled into its final geometry. Achieving a uniform temperature distribution is critical: excessive heating leads to thinning, while insufficient heating results in cracks and surface defects. Radiative heaters are commonly arranged above the sheet, and their power levels and positions must be tuned to produce a target temperature field.

Accurate modelling of the heating stage requires capturing conduction through the sheet, convection to the environment and diffuse-grey radiative exchange between heaters and the sheet. Since radiant flux depends on the fourth power of temperature and varies with geometrical view factors [1], high-fidelity numerical models must solve coupled conduction, convection and radiation equations to predict temperature distributions inside the oven.

Finite-element (FE) and computational fluid dynamics (CFD) simulations can capture these coupled phenomena, but they require fine meshes and ray-tracing algorithms to resolve steep gradients and non-linear boundary conditions. Consequently, each simulation may take hours, which is prohibitive when many design iterations or real-time control actions are needed. Recent work therefore turns to surrogate models—reduced-order or machine-learning approximations trained on high-fidelity data—to emulate the input–output behavior of the thermal system. Surrogates can be embedded in Digital twins, which go beyond static digital models or one-way digital shadows by enabling two-way data flow between the physical system and its virtual representation [2, 3]. In a true digital twin, adjustments made in the virtual model (for instance heater temperature settings) are applied to the physical asset, and sensor data from the asset continuously update the virtual model.

Several studies have addressed the estimation of sheet and heater temperatures in thermoforming. Throne investigated various heater array configurations to evaluate their influence on radiative heat transfer [4]. Nam *et al*. conducted a three-dimensional numerical analysis to explore the effects of zonal heating, where different heater elements operate at distinct temperature settings [5]. Ragoubi *et al*. implemented a simplified thermal mapping of the sheet to estimate its deformation during the forming stage [6]. Hosseinionari *et al*. proposed a computationally efficient approach that replaces a full 3D model with a calibrated 2D representation, reducing computational demands without resorting to reinforcement learning techniques [7]. Despite these advancements, none of the previous studies on thermal modeling in thermoforming have utilized machine learning models capable of achieving nearly an order of magnitude (≈10×) improvement in computational speed, as demonstrated in the present work.

Machine-learning surrogates have shown promise in replacing expensive FE/CFD solvers for steady-state heat transfer. In multi-plate clutch systems, Gaussian process and back-propagation neural network surrogates trained on FE data provide accurate thermal predictions and enable real-time evaluation [8]. Physics-informed neural networks (PINNs) enforce mass, momentum and energy balances directly in the loss function; when applied to integrated thermofluid systems they achieve relative errors below 1% and deliver predictions 75–88 times faster than conventional process models [9]. For impinging-jet configurations, surrogate models predict local Nusselt distributions with low error and orders-of-magnitude speed-ups versus CFD [10]. Surrogate modelling has also advanced for convection problems: a data-driven CNN–deconvolutional network uses signed distance functions to represent complex geometries and predicts steady-state heat convection fields four orders of magnitude faster than CFD, generalizing from simple training shapes to arbitrary test geometries [11]. In heat-exchanger design for electrified aircraft, a U-net trained on steady-state Navier–Stokes solutions predict velocity, pressure and temperature fields of finned heat exchangers with ~95% accuracy and low single-digit errors on pressure drop and temperature difference, supporting rapid optimization of heat-exchanger layouts [12]. Similarly, convolutional neural networks for steady laminar flow achieve real-time velocity predictions two orders of magnitude faster than a GPU-accelerated CFD solver and four orders faster than a CPU-based solver [13].

Conduction-dominated problems have likewise benefited from machine-learning surrogates. A physics-driven convolutional neural network (PD-CNN) maps geometric and loading parameters directly to the steady-state temperature field of a plate and couples with a particle-swarm optimization algorithm to identify optimal hole patterns for thermal management; the surrogate yields near-real-time predictions consistent with finite-element solutions [14]. Fully convolutional networks trained on randomly generated three-dimensional electronic systems approximate the complete steady-state temperature field with a mean relative error around 2% and evaluation times of about 35 ms per sample [15]. In industrial paint-curing ovens, machine-learning surrogates replace expensive CFD evaluations, enabling rapid exploration of design parameters and objective functions [16]. A physics-informed autoencoder reconstructs entire steady-state temperature fields from sparse sensor measurements with a relative average error of roughly 1.1%, outperforming Kriging and remaining robust when measurement data are scarce [17]. Outside of thermoforming, surrogate models have been applied to thermal analysis of traction motors; hybrid approaches combining analytical formulas with numerical simulations strike a balance between speed and fidelity, highlighting the importance of efficient surrogates for iterative design [18].

These examples demonstrate that steady-state heat-transfer surrogates—ranging from Gaussian processes and fully convolutional networks to physics-informed architectures—can provide high accuracy while reducing computational cost by orders of magnitude. Despite these advances, no prior study has combined high-fidelity Finite Element Method (FEM) data with a CNN surrogate to model radiative heating in thermoforming. Such a model could provide accurate temperature predictions with low latency, enabling instance digital twins for real-time control. The present work addresses this gap by training a fully convolutional neural network on a comprehensive FEM dataset to predict steady-state temperature fields in thermoforming, assessing its performance and demonstrating its potential for inverse optimization and fault-tolerant control.

2. Methods

2.1. Finite-element Simulation

All training data were generated numerically with the help of finite-element modelling (FEM). The FEM setup adopted here is consistent with the authors' previous work on digital-twin modelling for thermoforming [19], ensuring methodological continuity and validating the simulation framework. The thermoforming heating stage was modelled using the open-source solver CalculiX [20]. Heater elements were represented by two-dimensional shell elements with prescribed heat fluxes, and the high-impact polystyrene (HIPS) sheet was discretized using 8-node brick elements.

Steady-state heat conduction in a solid with constant thermal conductivity and no internal heat generation is governed by Laplace's equation,

$$\nabla^2 T = 0 \tag{1}$$

which follows from Fourier's law when the transient term and volumetric heat sources vanish [1].

For radiative heat transfer (Q_{12}) between heater element and sheet, with emissivities ε_1 and ε_2 respectively, the following equation can be utilized.

$$Q_{12} = \frac{\sigma(T_1^4 - T_2^4)}{\frac{1-\varepsilon_1}{\varepsilon_1 A_1} + \frac{1}{A_1 F_{12}} + \frac{1-\varepsilon_2}{\varepsilon_2 A_2}} \tag{2}$$

where σ is the Stefan–Boltzmann constant, A_1 is area of the heater element, A_2 is area of the sheet (or of the mesh, in discretized systems), F_{12} is view factor of the heater element onto the sheet, T_1 denotes absolute temperature of the heater element and T_2 is absolute temperature of the sheet [1].

In the finite-element simulations Equation-1 was discretized over the sheet geometry and coupled to radiative boundary condition (Fig. **1**). Conductivity of HIPS material is defined as 0.22 W/m-K. Radiative exchange between the heaters and sheet was modelled using diffuse-grey view factors ($\varepsilon_1 = \varepsilon_2 = 0.9$), and the net radiative heat flux

was computed from the Stefan–Boltzmann law with appropriate emissivities (Equation-2). Note that view factors between heater elements and cells on the sheet are calculated by CalculiX via numerical integration [20].

These boundary conditions yield a sparse linear system whose solution gives the steady-state temperature field for sheet at defined heater temperatures. Note that heater element temperatures are calculated with the help of temperature-wattage curve provided by the heater supplier.

Each heater element measured 100 mm × 100 mm, forming a 10 × 10 array that covered a total active heating area of 1 m². The polymer sheet had overall dimensions of 1000 mm × 1000 mm × 8 mm; however, due to symmetry boundary conditions, only half of the thickness (4 mm) was modeled to reduce computational cost. The distance between heaters plane and the sheet is defined as 200 mm. The finite-element mesh consisted of 21 × 21 × 3 nodes along the x, y, and z axes, respectively, providing sufficient spatial resolution to capture temperature gradients across the sheet.

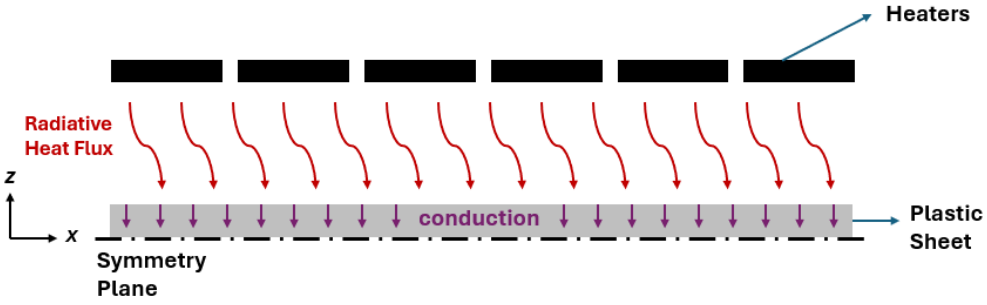

Figure 1: Problem definition.

2.2. Simulation Dataset

To generate a diverse dataset for training the neural-network surrogate, a series of finite-element simulations were performed under systematically varied heater-temperature distributions (Fig. **2**). Three representative configurations were considered: (i) uniform heating, where all heaters operated at constant temperatures between 300°C and 900°C; (ii) a single-hot-heater case, in which one localized element was assigned a higher temperature while the remaining heaters were kept at 300°C; and (iii) a single-cold-heater case, where one element was cooled relative to its neighbors. These scenarios enabled the model to capture both global and localized heat-transfer behavior, including hot-spot formation and cooling effects. Heater temperatures were incremented in 10°C steps to create a parametric sweep of boundary conditions, yielding a comprehensive set of steady-state temperature fields for training. The initial surrogate employed a four-layer multilayer perceptron (MLP) architecture with varying input size, trained using the Adam optimizer to minimize mean-squared error.

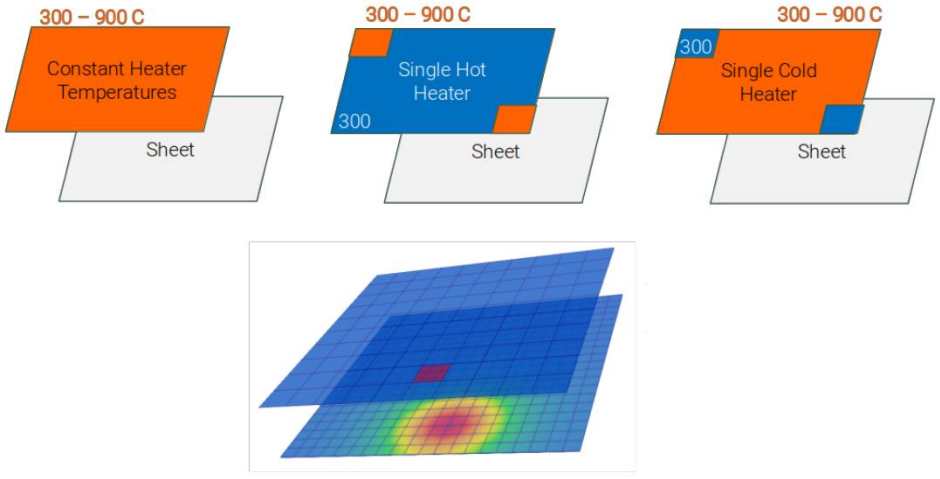

Figure 2: Schematic representation of FEM scenarios to create dataset.

2.3. Convolutional Neural Network Surrogate

To learn a mapping from process parameters to temperature fields, a fully convolutional neural network (CNN) was trained on the finite-element dataset. In each convolutional layer, a set of learnable filters slides across the input and, at every location, multiplies the filter coefficients with the corresponding input values and sums the products. For an input matrix (I) and filter (K), the output of the convolution at position (i,j) is

$$(I * K)(i,j) = \sum_{m=0}^{K_x-1} \sum_{n=0}^{K_y-1} I\,(i+m, j+n)\,K(m,n) \tag{3}$$

where K_x and K_y denote the filter dimensions. This operation is repeated for each filter and input channel to produce feature maps. Convolutional layers were interspersed with rectified-linear-unit activation functions, batch normalization and upsampling layers to map learned features back to the spatial domain.

The network input was a vector encoding heater temperature settings and sheet properties. This vector was reshaped to a format compatible with the convolutional layers and passed through the convolutional blocks described above. Network weights were optimized using the Adam algorithm with a learning rate of 10^{-3} and default momentum parameters. Training minimized the mean-squared error between the predicted and simulated temperatures. The dataset was split into training (80%), and test (20%) subsets, and early stopping was applied based on validation loss. After training, the surrogate reproduced FEM temperature fields with R^2 and a mean relative error of less than 3%. Each inference required less than 1 second, representing an 80–90% reduction in computation time compared with the finite-element solver. The differentiability of the surrogate also enabled gradient-based inversion for heater control.

2.4. Workflow Overview

The complete workflow used to generate data, train the surrogate and perform inverse optimization is summarized in Fig. (**3**). High-fidelity finite-element simulations of a 10 × 10 heater array were carried out with CalculiX, accounting for conduction through the sheet and diffuse-grey radiative heat transfer. For each simulation, the resulting steady-state temperature field was recorded on a 21 × 21 spatial grid. The dataset was then preprocessed by cleaning and scaling the inputs and outputs. Heater temperature vectors (100 inputs) and corresponding temperature fields were used to build the training and test sets via an 80/20 split. A convolutional neural network consisting of convolutional and dense layers was trained on the training set using the Adam optimizer and Huber loss with early stopping. The trained surrogate was validated on the test set by computing the mean absolute error and coefficient of determination. Finally, the differentiable surrogate was employed for gradient-based inverse optimization: heater temperatures were adjusted by backpropagating from a target temperature field to recover power distributions that produce the desired temperature profile.

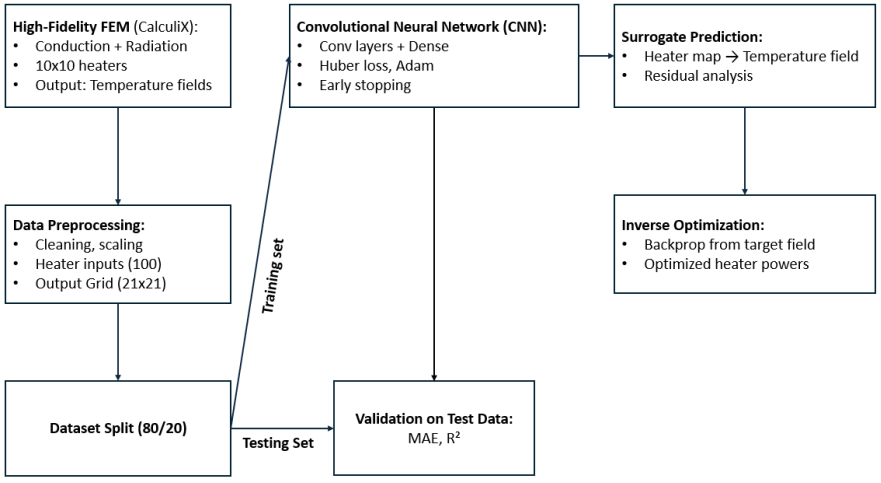

Figure 3: Workflow of the methodology.

2.5. CNN Architecture and Training Details

A convolutional neural network (CNN) architecture was adopted following standard practices for spatial surrogate modeling in radiative-heating problems. The network consisted of successive convolutional blocks combined with rectified linear unit (ReLU) activations and batch-normalization layers, which are widely used to stabilize training dynamics and accelerate convergence. The heater-temperature vector was reshaped into a 2D grid that reflects the spatial layout of the heater array; this approach preserves spatial correlations and enables convolutional layers to capture localized heating patterns more effectively than fully connected alternatives.

In the final implementation, the CNN surrogate consisted of four convolutional layers with 64, 128, 64, and 128 filters, respectively. The first convolutional layer used a 5×5 kernel to capture broader radiative-heating patterns, while the remaining layers employed 3×3 kernels to refine localized features. The network input dimension was 100, corresponding to the 10×10 heater-temperature vector, and the output dimension was 441, representing the predicted 21×21 steady-state temperature field. This configuration balances model capacity and computational efficiency, enabling accurate reconstruction of spatial temperature distributions while maintaining real-time inference capability.

The network was trained using the Adam optimizer with a standard learning-rate configuration (order of 10^{-3}), which provides robust convergence for convolution-based architectures. Default weight initialization (Xavier-type initialization) was employed, ensuring balanced propagation of activations without manual tuning. All input variables were normalized to the [0, 1] range to improve gradient stability and reduce training time. The Huber loss function was selected because of its robustness against local variations in FEM-generated temperature data. Training continued until the validation loss plateaued (Fig. **4**), and early stopping was used to prevent overfitting. This configuration provides a general and adaptable framework for surrogate modeling in thermoforming applications.

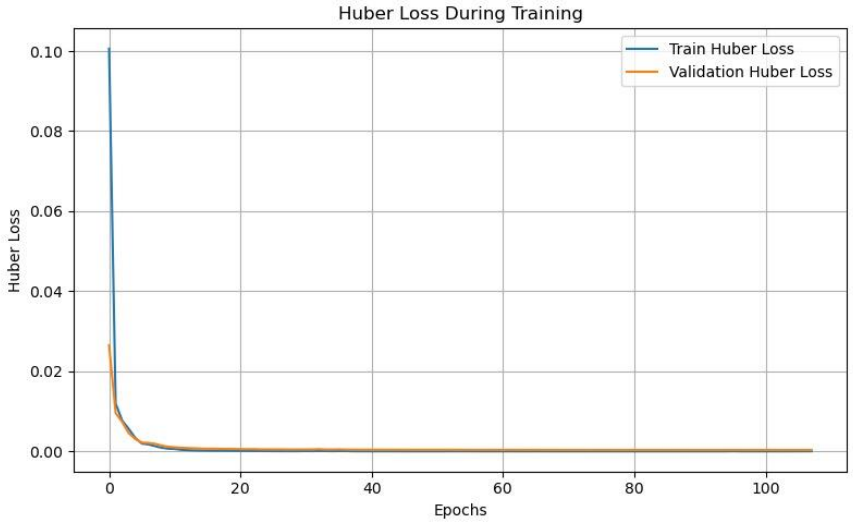

Figure 4: Training and validation Huber loss curves showing stable convergence of the CNN surrogate.

3. Results

3.1. Predictive Performance

The performance metrics used in this study follow the standard definitions of Mean Absolute Error (MAE) and the coefficient of determination (R^2). MAE quantifies the average magnitude of the prediction errors without considering their direction. It provides an interpretable measure of how much the CNN predictions deviate from the FEM temperatures on average. The coefficient of determination (R^2) measures the proportion of variance in the FEM temperatures that is explained by the CNN predictions. Values close to 1 indicate strong predictive performance and high fidelity to the reference simulations.

These metrics are calculated as follows:

$$MAE = \frac{1}{N}\sum_{i=1}^{N}|y_i - \hat{y}_i| \tag{4}$$

$$R^2 = 1 - \frac{\sum_{i=1}^{N}(y_i - \hat{y}_i)^2}{\sum_{i=1}^{N}(y_i - \bar{y})^2} \tag{5}$$

where y_i denotes the ground-truth temperature at node i obtained from the FEM simulations, $\hat{y}_i$ denotes the corresponding temperature predicted by the CNN surrogate, $\bar{y}$ represents the mean of all FEM temperatures in the dataset, N is the total number of spatial nodes used for performance evaluation.

The CNN surrogate was evaluated on a held-out test set of several hundred simulation cases. The surrogate achieved R^2, indicating that it explained more than 96% of the variance in the FEM temperature data. A parity plot of predicted temperatures by FEM versus CNN (Fig. **5**) shows that the points fall along the 45° line, demonstrating strong correlation. Error metrics further confirm the surrogate's accuracy: the mean absolute error was less than 3%. A histogram of pointwise errors (Fig. **6**) is tightly centered at zero, with all nodal temperatures within ±0.5% of the FEM values. The key performance metrics are summarized in Table **1**.

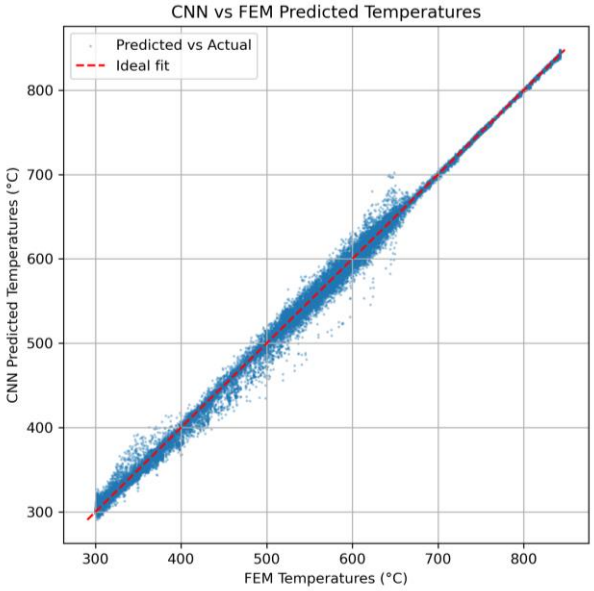

Figure 5: Predicted temperatures by FEM and CNN.

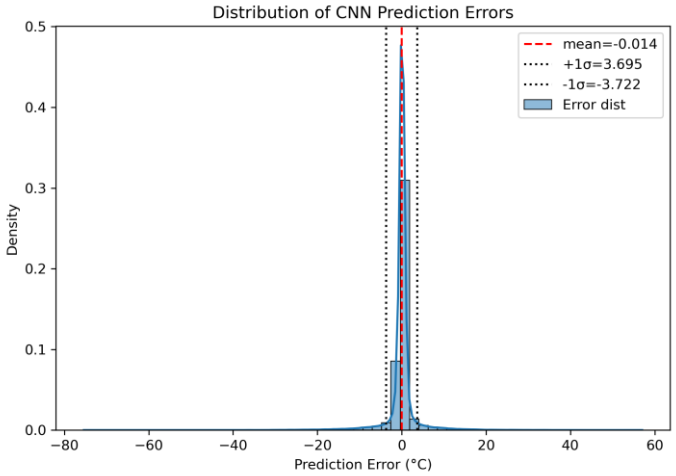

Figure 6: Distribution of pointwise prediction errors.

Table 1: Performance metrics of the CNN surrogate model.

Metric	Value
Coefficient of determination R^2	0.96
Mean absolute error (MAE)	<3%
Nodal temperatures within ±0.5%	100%
Inference time per case	<1 s
Speedup over FEM solver	7.7x

These metrics confirm that the surrogate accurately captures the nonlinear thermal response of the sheet.

3.2. Spatial Accuracy and Visualization

Spatial fidelity was assessed by comparing full temperature fields predicted by the surrogate with those computed by the FEM solver. Fig. (**7**) shows a representative example: the FEM ground truth, the surrogate prediction and the residual map. The CNN captures the location and magnitude of hot spots induced by high-power heaters as well as the smoother gradients resulting from conduction and radiative coupling. Residuals are confined to regions with steep gradients or near boundaries, illustrating that the surrogate preserves the spatial structure of the temperature field.

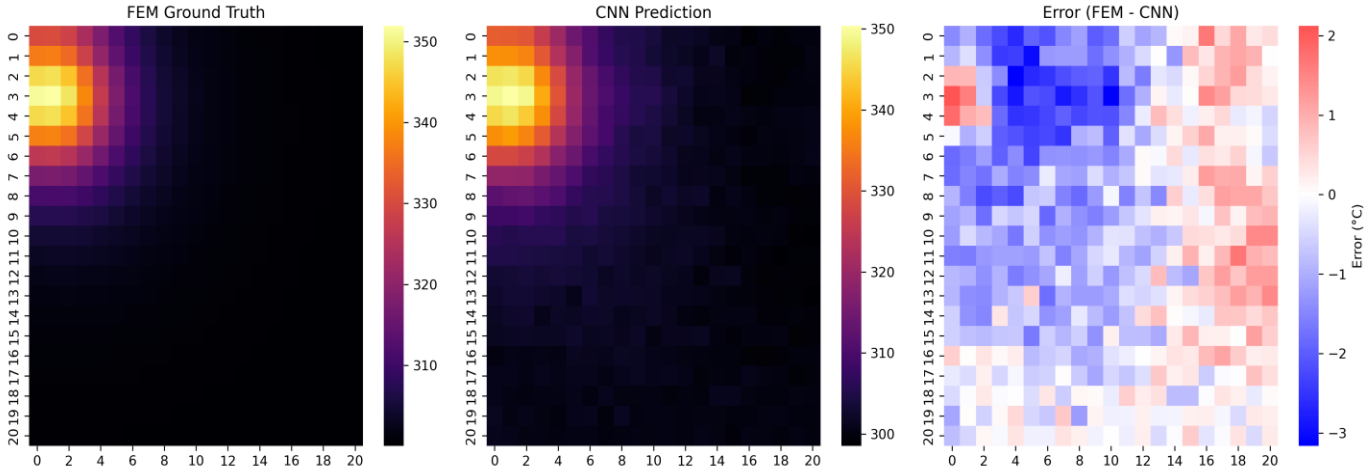

Figure 7: Comparison of FEM temperature field, CNN prediction and residual error.

3.3. Computational Efficiency

Each FEM simulation required on average 6.5 s of CPU time where simulation run times vary between 6 and 7 seconds. In contrast, the trained CNN produced a temperature field in under 1 s even on modest hardware. Fig. (**8**) compares the average computation time per case for the FEM solver and the surrogate. Although network training incurs an upfront cost, this expense is amortized over many evaluations. The surrogate therefore enables near-real-time exploration of heater settings, facilitating iterative optimization and process control.

Compared with alternative surrogate strategies such as fully connected artificial neural networks (ANNs) or physics-informed neural networks (PINNs), the CNN architecture provides a favorable balance between computational cost and predictive accuracy. Because CNNs inherently exploit spatial structure, they require fewer parameters than ANNs for equivalent performance and avoid the complex PDE-penalty terms used in PINNs. Reported literature trends for thermal surrogate modeling also show that CNN-based models generally achieve substantial reductions in evaluation time relative to FEM solvers, consistent with the speedup observed in this study.

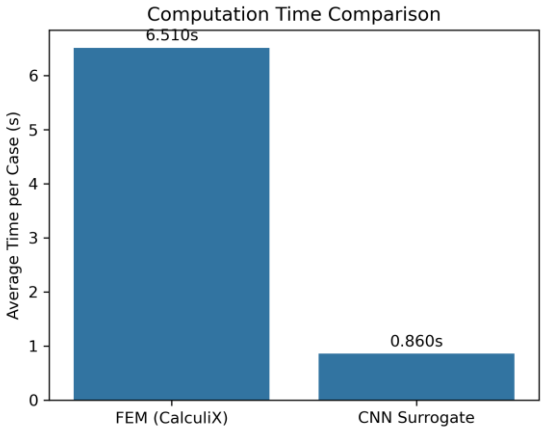

Figure 8: Comparison of average computation time per case for the FEM solver and the CNN surrogate.

3.4. Inverse Optimization and Fault Tolerance

The trained CNN is differentiable with respect to its inputs and can be used to solve inverse problems—determining heater settings that produce a specified temperature field. A gradient-based optimization procedure minimized the mean-squared error between the surrogate prediction and a target temperature map, updating heater temperatures subject to physical limits. Fig. (**9**) illustrates a case where the original heater temperatures were successfully recovered from a target temperature field. When the reconstructed heater distribution was re-simulated using the FEM model, the resulting temperature field matched the target closely, validating the inversion approach.

To assess robustness, the inversion was repeated with one heater element constrained to low power to mimic an actuator failure. Fig. (**10**) shows that the optimizer reallocates power among the remaining heaters to compensate, yielding a temperature distribution very close to the target. This demonstrates that the surrogate can support fault-tolerant control strategies—an essential requirement for industrial deployment.

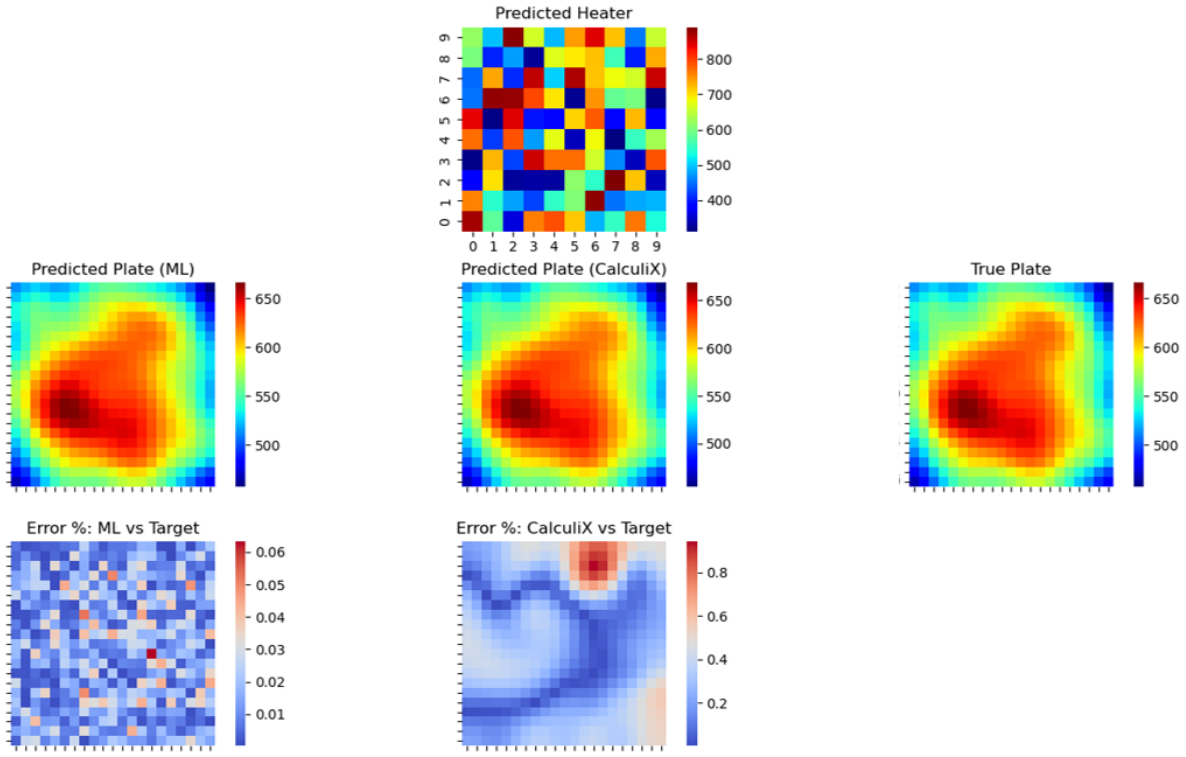

Figure 9: Inverse optimization: target and predicted temperature fields and recovered heater temperatures.

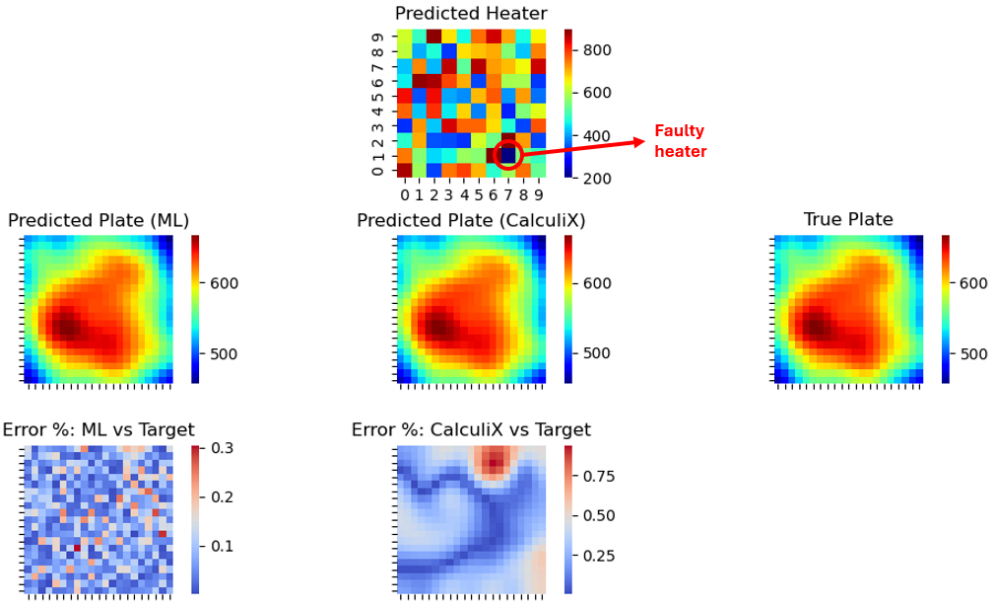

Figure 10: Fault-tolerant optimization with a failed heater element.

The inverse-optimization problem was formulated as minimizing the discrepancy between the CNN-predicted and target temperature fields. This was achieved through gradient-based updates applied directly to the heater-temperature vector, exploiting the differentiability of the surrogate model. Physical bounds on allowable heater temperatures were enforced during optimization. This general formulation enables the system to automatically redistribute heat loads when a heater fails, illustrating the suitability of the approach for real-time digital-twin control and fault-tolerant operation.

4. Discussion

This study demonstrates the feasibility of applying a convolutional-neural-network surrogate to the steady-state heating stage of thermoforming. By training on high-fidelity FEM data, the surrogate successfully captured the nonlinear relationship between heater temperature distributions and resulting temperature fields. The model reproduced FEM predictions with high accuracy (R^2=0.96, error<3%) while providing an order-of-magnitude reduction in computation time, thereby making real-time evaluation and control realistic for industrial deployment. Importantly, the differentiability of the surrogate enabled gradient-based inversion, which not only recovered optimal heater settings but also compensated for heater failures. These capabilities underline the potential of surrogate models to bridge the gap between high-fidelity simulation and practical digital-twin control.

Despite these strengths, certain limitations must be acknowledged. The surrogate relies exclusively on synthetic FEM data under steady-state assumptions, whereas industrial thermoforming often involves transient heating dynamics and uncertain boundary conditions. Experimental calibration—e.g., through infrared thermography—would be valuable for validating the model against real manufacturing data. Future extensions should also explore transient simulations, integrate uncertainty quantification, and expand to more complex three-dimensional geometries. Furthermore, embedding physics-informed constraints or hybrid architectures could improve generalizability, reduce data requirements, and increase robustness under noisy measurements. By addressing these challenges, CNN surrogates can evolve into reliable engines of real-time optimization within digital-twin frameworks, ultimately advancing thermoforming toward first-time-right production and fault-tolerant operation.

5. Conclusion

This study presents a convolutional-neural-network surrogate that effectively reproduces high-fidelity FEM predictions of radiative heating in thermoforming while reducing evaluation time from seconds to milliseconds.

The surrogate achieves high accuracy ($R^2 \approx 0.96$, <3% error) and, through its differentiability, enables gradient-based inverse optimization and fault-tolerant heater control. These capabilities transform high-fidelity simulations into actionable tools for real-time decision-making.

Data-driven CNN architectures offer an effective way to approximate steady-state radiative heating behavior when trained on high-fidelity FEM datasets. The approach does not rely on explicit PDE constraints, as in PINNs, which simplifies implementation while maintaining high predictive accuracy. The methodology remains general and flexible, allowing adaptation to different thermoforming geometries and boundary conditions. Future work may incorporate experimental calibration or physics-informed extensions to further increase robustness.

Beyond the immediate gains in computational efficiency, the results demonstrate how machine-learning surrogates can be embedded into digital-twin frameworks to enable first-time-right production, reduce material waste, and improve operational robustness. By extending this approach to transient dynamics, experimental validation, and more complex geometries, CNN surrogates can evolve into a general methodology for real-time optimization across thermoforming and other thermally driven manufacturing processes. The work therefore not only advances thermoforming research but also contributes to the broader agenda of physics-informed AI for industrial digital twins.

Conflict of Interest

The authors declare no conflicts of interest.

Funding

This research has been supported by the ZDZW (Zero Defect Zero Waste) project. The ZDZW project has received funding from the European Union's Horizon Europe programme under grant agreement No 101057404. Views and opinions expressed are however those of the author(s) only and do not necessarily reflect those of the European Union. Neither the European Union nor the granting authority can be held responsible for them.

Acknowledgements

The authors thank Horizon Europe Programme for funding these research efforts.

References

[1] Incropera FP, DeWitt DP, Bergman TL, Lavine AS. Fundamentals of heat and mass transfer. 6th ed. Hoboken (NJ): John Wiley & Sons; 2007.

[2] Díaz Sierra EF, Cruz De Jesus FM, Jiménez José JJ, Lebrón Santana A, Nuñez Ríos JJ, Traverso Avilés LM. Machine learning surrogate dynamical system model for thermal energy storage. LACCEI Int Multi-Conf Eng Educ Technol. 2024; 1(1): 1795. https://doi.org/10.18687/LACCEI2024.1.1.1795

[3] Johnston G. Digital Twins. The Case for Policy Use. Energy Systems Catapult; 2023.

[4] Throne JL. Radiant heat transfer in thermoforming. SPE ANTEC Tech Papers. 1995; 41: 000.

[5] Nam GJ, Ahn KH, Lee JW. Three-dimensional simulation of thermoforming process and its comparison with experiments. Polym Eng Sci. 2000; 40(10): 2232-40. https://doi.org/10.1002/pen.11355

[6] Ragoubi A, Ducloud G, Agazzi A, Dewailly P, Le Goff R. Modeling the thermoforming process of a complex geometry based on a thermo-visco-hyperelastic model. J Manuf Mater Process. 2024; 8(1): 33. https://doi.org/10.3390/jmmp8010033

[7] Hosseinionari H, Ramezankhani M, Seethaler R, Milani AS. Development of a computationally efficient model of the heating phase in thermoforming process based on the experimental radiation pattern of heaters. J Manuf Mater Process. 2023; 7(1): 48. https://doi.org/10.3390/jmmp7010048

[8] Schneider T, Beiderwellen Bedrikow A, Dietsch M, Voelkel K, Pflaum H, Stahl K. Machine learning based surrogate models for the thermal behavior of multi-plate clutches. Appl Syst Innov. 2022; 5(5): 97. https://doi.org/10.3390/asi5050097

[9] Laugksch K, Rousseau P, Laubscher R. A PINN surrogate modeling methodology for steady-state integrated thermofluid systems modeling. Math Comput Appl. 2023; 28(2): 52. https://doi.org/10.3390/mca28020052

[10] Tahmasebi Moradi A, Ren V, Le-Creurer B, Mang C, Yagoubi M. Feasibility study of CNNs and MLPs for radiation heat transfer in 2-D furnaces with spectrally participative gases. arXiv preprint arXiv:2506.08033. 2025.

[11] Peng JZ, Liu X, Aubry N, Chen Z, Wu WT. Data-driven modeling of geometry-adaptive steady heat transfer based on convolutional neural networks: heat convection. arXiv preprint arXiv:2101.03692. 2021. https://doi.org/10.3390/fluids6120436

[12] Bokil G, Geyer TF, Wolff S. Towards convolutional neural networks for heat exchangers in electrified aircraft. In: Proceedings of the Deutscher Luft- und Raumfahrtkongress 2023; October 2023; Stuttgart, Germany. https://doi.org/10.2514/6.2024-4108

[13] Guo X, Li W, Iorio F. Convolutional neural networks for steady flow approximation. In: Proceedings of the 22nd ACM SIGKDD International Conference on Knowledge Discovery and Data Mining (KDD '16). San Francisco, CA, USA; 2016 Aug 13-17. p. 481-90. ACM. https://doi.org/10.1145/2939672.2939738

[14] Sun Y, Elhanashi A, Ma H, Chiarelli MR. Heat conduction plate layout optimization using physics-driven convolutional neural networks. Appl Sci. 2022; 12(21): 10986. https://doi.org/10.3390/app122110986

[15] Stipsitz M, Sanchis-Alepuz H. Approximating the steady-state temperature of 3D electronic systems with convolutional neural networks. Math Comput Appl. 2022; 27(1): 7. https://doi.org/10.3390/mca27010007

[16] Parsons Q, Nowak D, Bortz M, Johnson T, Mark A, Edelvik F. Machine learning surrogates for the optimization of curing ovens. Eng Appl Artif Intell. 2024; 133(Pt C): 108086. https://doi.org/10.1016/j.engappai.2024.108086

[17] Sabathiel S, Sanchis-Alepuz H, Wilson AS, Reynvaan J, Stipsitz M. Neural network-based reconstruction of steady-state temperature systems with unknown material composition. Sci Rep. 2024; 14: 22265. https://doi.org/10.1038/s41598-024-73380-1

[18] Fiala V, Pechánek R. Surrogate-based heat transfer modeling for important parts in a fully enclosed traction motor. Exp Therm Fluid Sci. 2025; 107: 9649–62. https://doi.org/10.1007/s00202-025-02993-0

[19] Turan E, Konuşkan Y, Yıldırım N, Tunçalp D, İnan M, Yasin O, *et al*. Digital twin modelling for optimizing the material consumption: a case study on sustainability improvement of thermoforming process. Sustain Comput Inform Syst. 2022; 35: 100655. https://doi.org/10.1016/j.suscom.2022.100655

[20] Dhondt G. The finite element method for three-dimensional thermomechanical applications. Hoboken (NJ): Wiley; 2004. https://doi.org/10.1002/0470021217